Theoretical and Computational Acoustics

Nejma Chahine

November 6, 2023

1 Introduction

Our objective with this second stage is to utilize the mesh generated in the previous report to compute acoustic waves within a predefined boundary. We will be to numerically solve Partial Differential Equations (PDEs) and try to conclude on the effect of different geometrical and physical properties on the propagation of the wave.

2 General overview

in this first part we will discuss the current system and how we will be solving the helmholtz equation.

2.1 Helmholtz equation

$$\Delta u + k^2 u = f, in\, \Omega \tag{1}$$

Here, Ω represents a two-dimensional domain described as $\Omega = [0,1] \times [0,1]$, and its boundary is partitioned into two disjoint sets, Γ_d and Γ_n, where Γ_d denotes the left boundary. The boundary conditions associated with this problem are given as follows:

- Dirichlet condition: $u = 0, on\, \Gamma_d$
- Neumann condition: $\frac{\partial u}{\partial n} = 0, on\, \Gamma_n$

meaning that on the left boundary we have perfect sound insulation.this system will be solved on the following comb-like meshes:

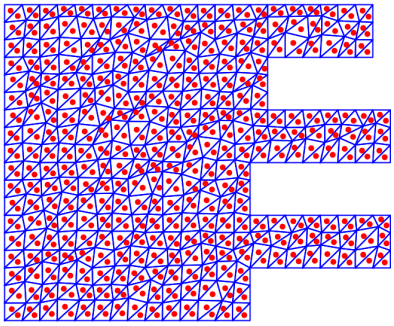

Figure 1: Disturbed comb-like mesh

2.2 solving the equation

in the file solve.py we have an exemple of the process that we are conducting to get the appropriate functions that model the acoustic wave. WE have **resolve_eq(p_e2n, e2n, node_coords,f_unassembled,values_on_boundary,frequency=2)** which takes in a mesh and a frequency and through the finite difference method gets the matrix **A** and the discreat solution for the equation .**A** represents the first part of the helmholtz equation (i.e **A** is independent of the excitation of the second part of the equation) in the given mesh. from **A** we get the eigenvalues and eigenvectors which permits us to solve for stationary waves in different systems. for different geometries and for different absorbtion rates inside the materials we get different eigen values that we represent here:

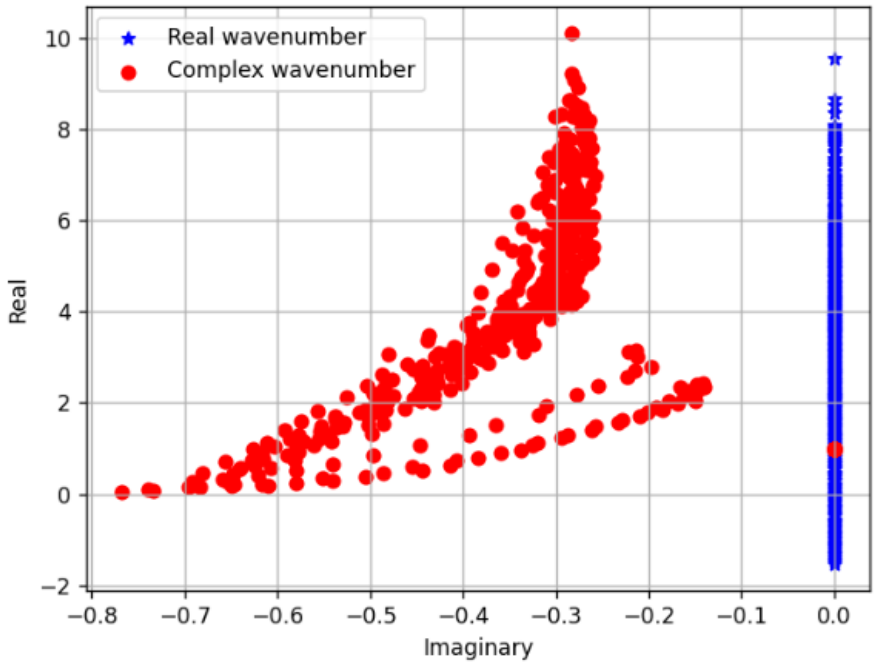

Figure 2: eigen-values for the void and absorbing materials

during this first part we have an essential part of the modeling process , since we can not find an explicit solution for all the geometries (thus our interest in this numerical analysis) we compare our results on a simple system with the real function. getting adequate results comparable to the real function is essential to trust the following results.

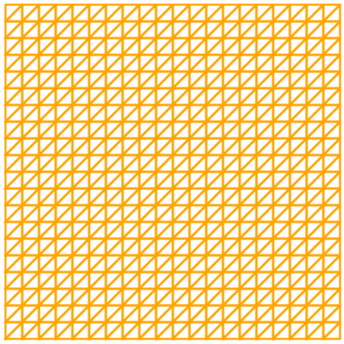

Figure 3: simple testing mesh

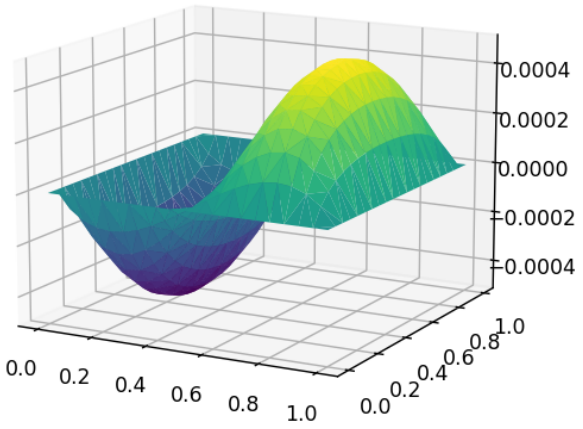

Figure 4: real error between modeled and theoretical results

from the amplitude of the graph we can see that the error can be neglected. As you can see we have two bulges for the error which indicates that this graph is highly dependent not only to the step but also to the frequency. will dive further in our understanding of the error in the next section

3 Pollution and dispersion error of the finite element method

In this section, we aim to compute the finite element solution u_h for various combinations of step sizes h and wave-numbers k. We will consider a particular case where an exact solution u^* is available. To assess the accuracy of our numerical solution, we will compute the error, which measures the difference between the exact solution u^* and the finite element solution u_h. This error analysis will provide insights into the convergence and reliability of our numerical method.
The outcomes of this investigation will not only contribute to a deeper understanding of the Finite Element Method but will also assist in making informed choices about mesh size selection in real-world applications, ensuring the attainment of accurate and reliable solutions in engineering and scientific domains.

3.1 effects of the step h

The theoretical result of the finite element method indicates that the error can be bounded by $C \cdot h^{\alpha}$, where α represents the convergence rate. The purpose of this study is to evaluate the value of α and, furthermore, to illustrate how the error (err) changes as the mesh size (h) varies.
To estimate α, we will employ a logarithmic approach by taking the natural

logarithm of the error equation, and we will compute the error for different geometries through.
the regression seems to be adequate for both cases of ordered and undordered meshs which indicates that $\alpha = 1.7$

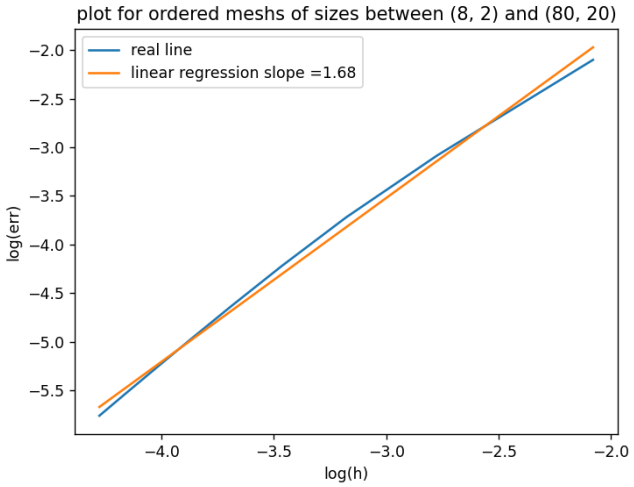

Figure 5: linear regression on ordered meshs

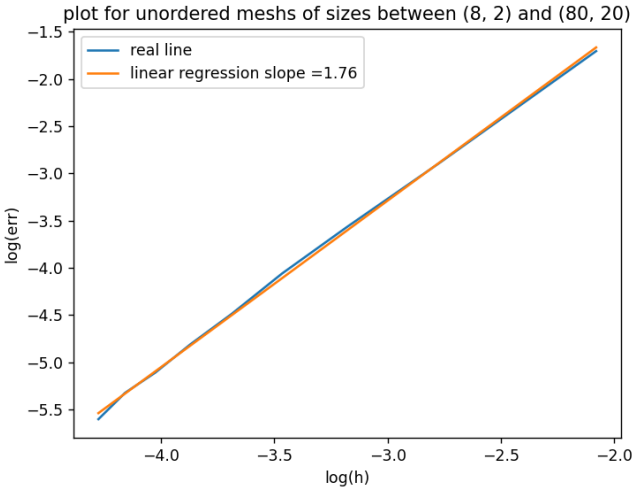

Figure 6: linear regression on unordered meshs

3.2 effects of the wavenumber K

Similarly, The theoretical result of the finite element method indicates that the error can be bounded by $C_k \cdot k^{\beta}$, where β represents the convergence rate. The purpose of this study is to evaluate the value of β and, furthermore, to illustrate how the error (err) changes as the wave-number (K) varies.
To estimate β, we will employ a logarithmic approach by taking the natural logarithm of the error equation, and we will compute the error for different geometries

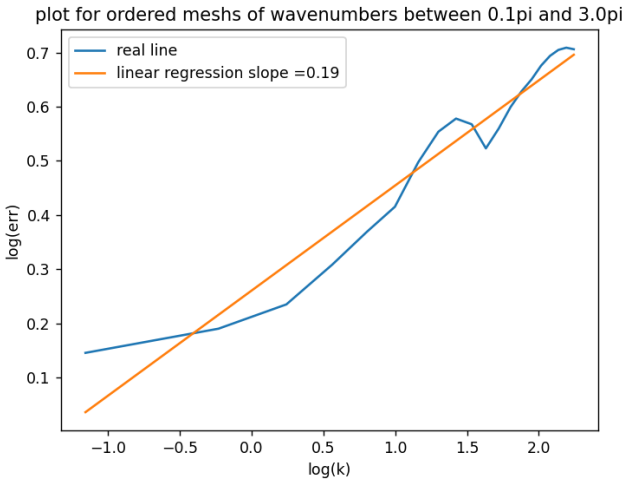

Figure 7: linear regression on ordered meshs

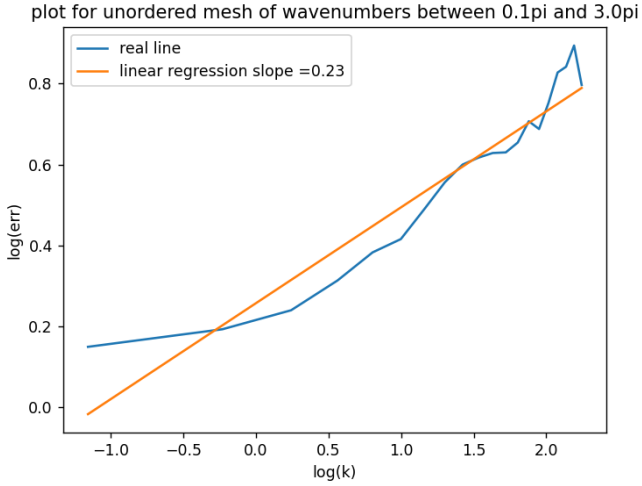

Figure 8: linear regression on unordered meshs

the relationship between k and the error exhibits a positive correlation however we do not get a proper linear relationship, this indicates that we are underestimating β . since in theory we have a inequality we can confirm that $\beta > 0.23$

3.3 discussion on the difference between ordered and unordered meshs

First of all, it is important to consider the impact of how we perturbed the nodes on our ability to estimate the average length of the new edges. In our procedure, we displaced the nodes by a vector of a randomly chosen length, following a uniform distribution ranging from 0 to half the length of the initial edge. The direction of the vector was also determined by a uniform distribution. As a result, we can estimate that $\mathbf{E(new\ edge) = \sqrt{\frac{9}{8}}\ old\ edge = 1.060\ old\ edge}$. This estimation suggests that on sufficiently large meshes, the average length of steps will closely approach the expected value. In this process, we take the natural logarithm of the step length, which means there is no need to modify our approach when testing unordered meshes. However it is important to note that the random process creates a higher variance while computing and the results for both α and β differ quite a lot between computations.

4 Control of acoustic wave by changing the geometry on a surface

in this section we will explore our numerical approach on the comb-like mesh introduced previously. we will try to understand the influence of the shape in

the localisation of the wave.

4.1 effect of the frequency

we will discuss the effect of the frequency on this first mesh with relatively large peaks

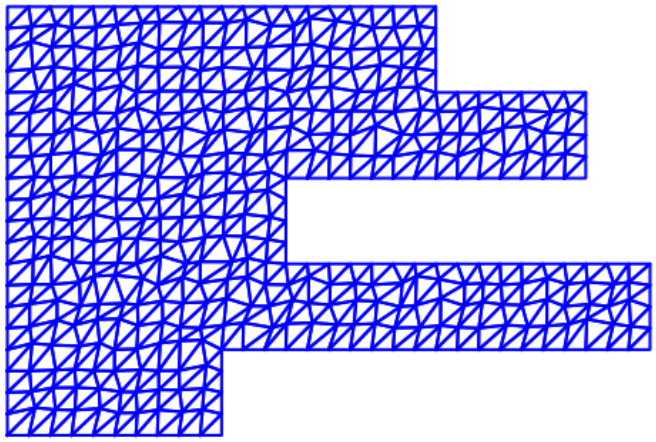

Figure 9: Enter Caption

first we will visualise the eigen-modes on the mesh, to do this we will assign to the second member of the equation the eigen-vectors of the matrix A, where A represents ,as we said earlier, the first part of the equation and the geometry. we will see eigen-modes for wave lenghths of { 0.5, 2, 100}

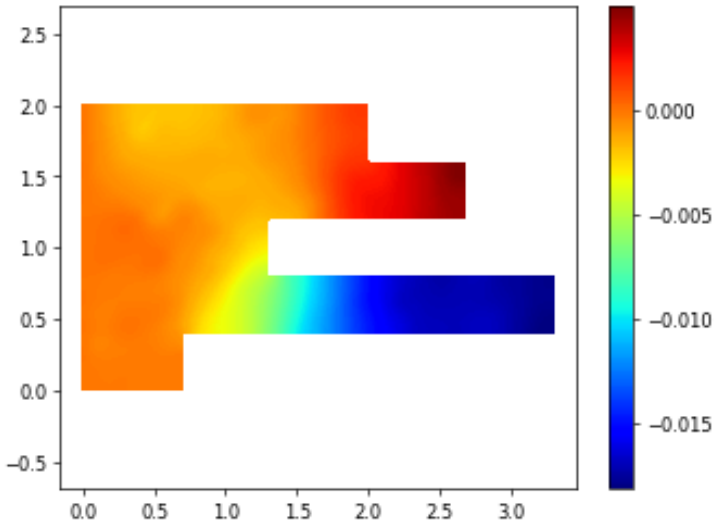

Figure 10: propagation of wave with a wavelength of 100

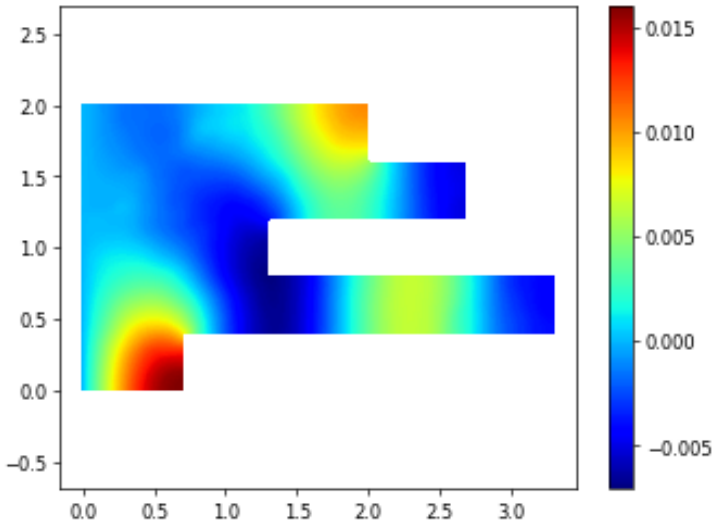

Figure 11: propagation of wave with a wavelength of 2

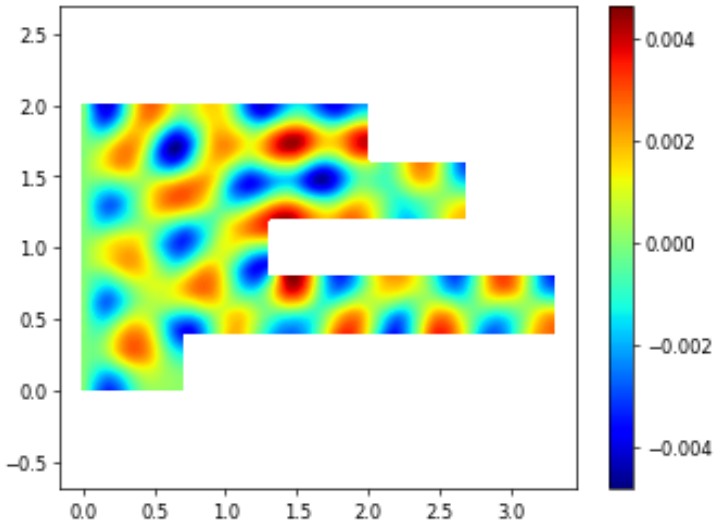

Figure 12: propagation of wave with a wavelength of 0.5

as we cann see we have the left boundary equal to zero and we have no variance of the value perpendicular to other surfaces which indicates that our process was conclusive and that we have the appropriate eigen-modes.
on the last figure with the smallest wavelength we can clearly see that we have nodes and peaks which indicates a standing wave. w can also see that for the smaller wavelength we have better penetration of the wave inside the complex geometry which is reminicent of the effect of absorbing walls in class.

4.2 eigenmodes localizing inside this geometry

in the file solve.py we have a function **calcule_surface_existence(solreal)** that calculates the existence surface:

$$S_j = \frac{1}{R} \int_\Omega |\phi_j|^4 \, dxdy$$

subject to the condition:

$$\int_\Omega |\phi_j|^2 \, dxdy = 1$$

as well as **calcule_energie_dissipation(solreal,node_coords, p_elem2nodes, elem2nodes)** that returns the energy dissipation:

$$w_j = \int_\Gamma |\phi_j|^2 \, d\sigma$$

we calculate both existence surface and energy dissipation for all the eigen-modes and we sort them to get a panel of the most and least localizing modes according to the existence surface criterion we get as exemples:

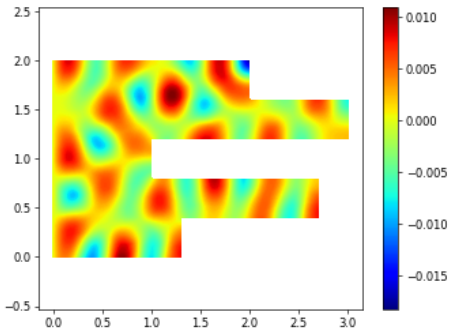

Figure 13: exemple of localizing mode

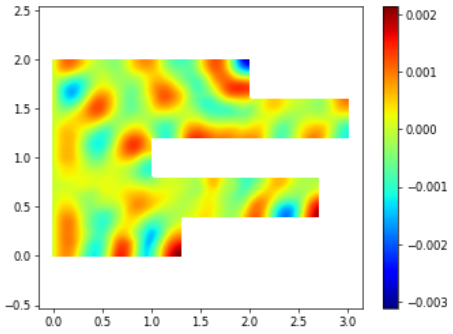

Figure 14: exemple of unlocalizing mode

according to the energy dissipation criterion we get as exemples:

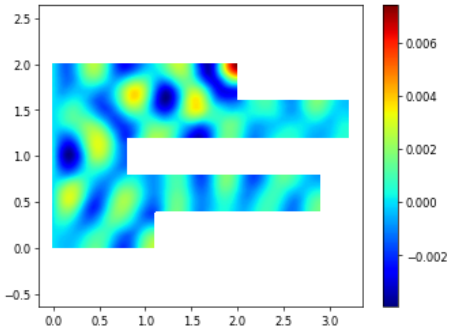

Figure 15: exemple of localizing mode

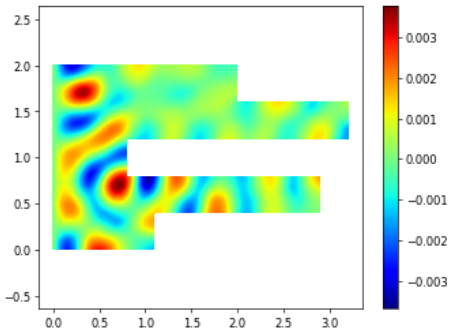

Figure 16: exemple of unlocalizing mode

4.3 effect of the frequency on more extreme geometries

for the next subsections we will look at the following mesh, as we can see we have a higher number of thin peaks.

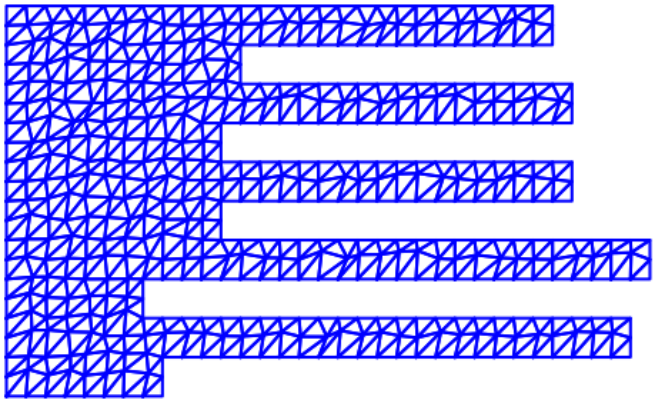

For this geometry, and depending on the mode we choose, we can observe that even for shorter wavelengths, the waves still encounter difficulty propagating inside the peaks, as illustrated here:

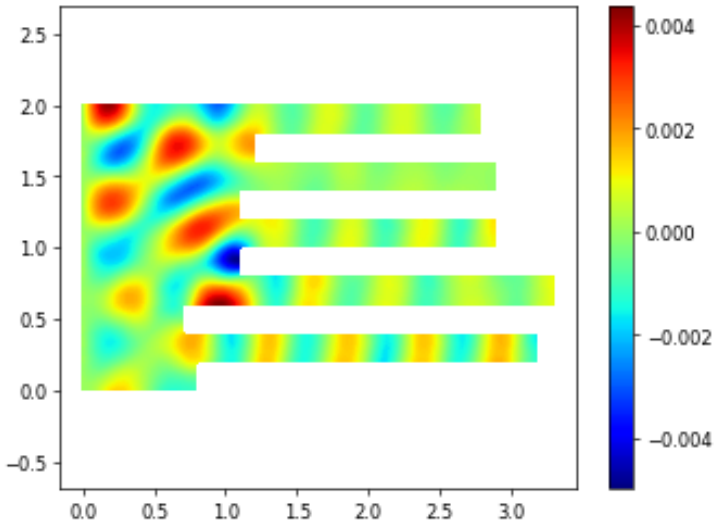

Figure 17: propagation of a wave with a wevelength of 0.5

4.4 eigenmodes localizing inside this geometry

in a similar way we look at the localization of the modes whith the existanc surface criterion

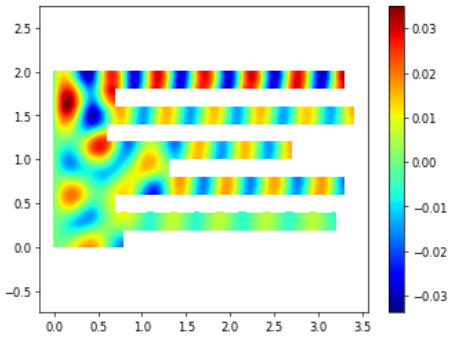

Figure 18: exemple of localizing mode

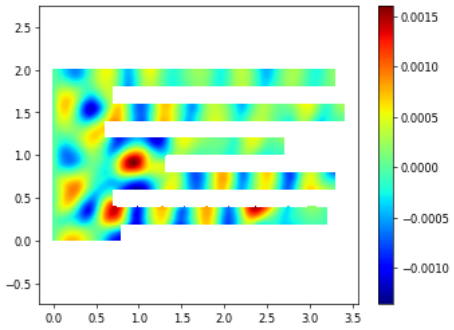

Figure 19: exemple of unlocalizing mode

4.5 Existence surface for different cavities

for this last part we look at the existence surface for different geometries , a more typical approach would have been to compare $\frac{S_n}{S}$ but since we are conserving the volume of the mesh we plot the existence surface for each eigen value. As we can see typically the first geometry localizes less than the second one which is aligned with the fact that the waves get traped outside the peaks and can not penetrate as easily

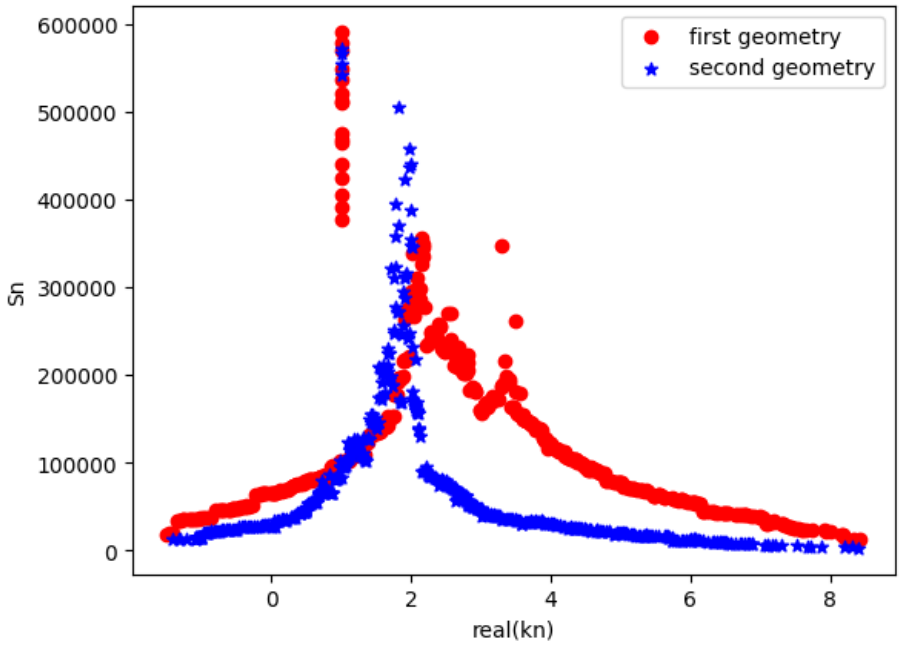

Figure 20: existence surface for different geometries

5 conclusion

In conclusion, our study has focused on understanding the model's behavior concerning the variation of model parameters, equations, and geometry. We have thoroughly examined the model's responses to these modifications to gain a deeper insight into its behavior under diverse conditions. These investigations have enhanced our understanding of the influences of parameters and geometry on the outcomes, thereby strengthening our ability to use the model judiciously in a wide range of contexts.